AAEC/E490

AAEC/E490

AUSTRALIAN ATOMIC ENERGY COMMISSION

RESEARCH ESTABLISHMENT

LUCAS HEIGHTS

MEASUREMENT OF TIME-DEPENDENT FAST NEUTRON ENERGY SPECTRA IN A DEPLETED URANIUM ASSEMBLY

by

S. WHITTLESTONE

October 1980

ISBN 0 642 59700 6

AUSTRALIAN ATOMIC ENERGY COMMISSION
RESEARCH ESTABLISHGMENT
LUCAS HEIGHTS

MEASUREMENT OF TIME-DEPENDENT FAST NEUTRON ENERGY SPECTRA IN A DEPLETED URANIUM ASSEMBLY

by

S. WHITTLESTONE

ABSTRACT

Time-dependent neutron energy spectra in the range 0.6 to 6.4 MeV have been measured in a depleted uranium assembly. By selecting windows in the time range 0.9 to 82 ns after the beam pulse, it was possible to observe the change of the neutron energy distributions from spectra of predominantly 4 to 6 MeV neutrons to spectra composed almost entirely of fission neutrons. The measured spectra were compared to a Monte Carlo calculation of the experiment using the ENDF/B-IV data file. At times and energies at which the calculation predicted a fission spectrum, the experiment agreed with the calculation, confirming the accuracy of the neutron spectroscopy system. However, the presence of discrepancies at other times and energies suggested that there are significant inconsistencies in the inelastic cross sections in the 1 to 6 MeV range.

(Continued)

The time response generated concurrently with the energy spectra was compared to the Monte Carlo calculation. From this comparison, and from examination of time spectra measured by other workers using ^{235}U and ^{237}Np fission detectors, it would appear that there are discrepancies in the ENDF/B-IV cross sections below 1 MeV. The predicted decay rates were too far below and too high above 0.8 MeV.

National Library of Australia card number and ISBN 0 642 59700 6

The following descriptors have been selected from the INIS Thesaurus to describe the subject content of this report for information retrieval purposes. For further details please refer to IAEA-INIS-12 (INIS: Manual for Indexing) and IAEA-INIS-13 (INIS: Thesaurus) published in Vienna by the International Atomic Energy Agency.

DEPLETED URANIUM; NEUTRON SPECTRA; MEV RANGE 01-10; TIME DEPENDENCE; ENERGY SPECTRA; URANIUM 238; INELASTIC SCATTERING; CROSS SECTIONS; FISSION NEUTRONS; NEUTRON SPECTROSCOPY

CORRIGENDA

AAEC/E490 by S. Whittlestone

Abstract: In the penultimate line 'too far below' should read 'too low below'

Page 14: Cawley and Whittlestone [1980] ..... delete 'Submitted to'. Amend to Nucl. Instrum. Methods, 177:537.

Page 15: Rainbow [1980] ... insert 'Time-dependen ^{235}U and ^{237}Np fission rates in a depleted uranium assembly.'

Page 15: Whittlestone [1980c] ... delete 'Submitted to'. Amend to Nucl. Instrum. Methods, 173:347.

CONTENTS

1. INTRODUCTION 1

2. EXPERIMENTAL DESIGN 3

3. THE EXPERIMENTAL FACILITY 5
   3.1 The Neutron Source 5
   3.2 The Uranium Assembly 5

4. MEASUREMENT OF TIME-DEPENDENT NEUTRON ENERGY SPECTRA 6
   4.1 Introduction 6
   4.2 The Electronic System 6
   4.3 Calibrations 7
   4.4 The Experimental Data Collection System 8
   4.5 The Spectrum Measurement 8

5. RESULTS AND DISCUSSION 10
   5.1 Results 10
   5.2 Comparison of Experiment with Calculation and Fission Spectrum 11
   5.3 Comparison with Fission Detector Measurements 12

6. CONCLUSIONS 13

7. ACKNOWLEDGEMENTS 14

8. REFERENCES 14

Table 1 Composition of Depleted Uranium Blocks 17

Table 2 Specification of the Time-dependent Neutron Energy Spectrum Measurement 18

Table 3 Energy Boundaries for Regrouped Neutron Energy Spectra 19

Figure 1 Group inelastic scattering cross sections for ^{235}U 21

(Continued)

CONTENTS (Continued)

Figure 2 The scintillator probe 22

Figure 3 Schematic diagram of the uranium assembly and some associated facilities 23

Figure 4 Schematic diagram of the time-dependent neutron energy spectrum measurement system 24

Figure 5 Range and average % pile-up versus time after beam pulse 25

Figure 6 Time response of scintillation detector in uranium stack calculated by Monte Carlo code 25

Figure 7 Typical beam pulse time responses. Time window 1 starts at 8.9 ns 26

Figure 8 Original and regrouped neutron energy spectra from time window at 12 ns 26

Figure 9 Neutron energy spectra in uranium stack 1.9 to 12 ns after the beam pulse peak 27

Figure 10 Neutron energy spectra in uranium stack 14 to 34.5 ns after the beam pulse peak 28

Figure 11 Neutron energy spectra in uranium stack 39.6 to 77.2 ns after the beam pulse peak 29

Figure 12 Comparison of experimental and theoretical neutron energy spectrum shapes versus time after beam pulse peak 30

Figure 13 Neutron energy above which spectrum matches fission spectrum versus time after beam pulse peak 30

Figure 14 The relative efficiencies (a) and time spectra (b) of three detectors. Normalisation of all curves arbitrary 31

Appendix A Listing of FOCAL Program 'Walk' 33

Appendix B The Time-dependent Neutron Energy Spectra 35

1. INTRODUCTION

Fast reactors have operated successfully since 1952 and their technical feasibility is not in doubt. Their commercial acceptance will depend largely on their safety, reliability and economics. The economics in particular requires accurate quantitative prediction of the fast reactor's performance. The core and shield designs, and fuel management strategies demand an ability to calculate the neutronics of the system accurately. Most of the quantities required (power distribution, critical mass, breeding ratio, fuel burn-up and safety margins) are a function of the neutron spectrum which characterises the reactor. Numerical solution of the transport theory equations provides a reasonably accurate estimate of the spectrum provided that accurate neutron cross sections are available as input. Although significant improvements to the cross sections have generally been made, this has not been the case for the inelastic scattering cross section of ^{238}U. This cross section is a major influence in determining the fast reactor spectrum and accurate microscopic or differential measurements are difficult because of the presence of ^{238}U fission events. Errors in the inelastic scattering cross section of ^{238}U are thought to be in the range of 10 to 50 per cent [W. Gemmell, AAEC private communication].

Although claims have been made stressing the high economic costs of such uncertainties in the input data [Greebler et al. 1970], the practical realities are not so harsh because several fuel enrichments are generally used. Slight changes in the proportion of core allocated to a given enrichment and optimisation of fuel management substantially reduce the economic penalty. This is not to deny that uncertainties are undesirable and ways have to be examined of reducing them. Simple integral, homogeneous experiments can be designed which highlight spectrum-weighted, cross-sectional quantities and hence provide an upper limit to the uncertainties. These experiments are extremely valuable in clarifying the issues and the errors and in emphasising those areas in which greater accuracy is required.

The integral experiments used for testing data or calculational methods fall into three groups. One group measures stationary, or time-averaged, neutron spectra with spectrometers such as ^{3}He or proton recoil [Bluhm et al. 1974] or, with coarser resolution, using threshold foils [Kabir and Cooper 1972]. Other experiments in this group, which involve pulsing the test assembly with an intense source and separating out the energies by time-of-flight, have the advantage of inherent accuracy of time-of-flight techniques

but suffer the disadvantage of needing quite massive equipment [Ragan et al. 1976; Malaviya et al. 1972]. For example, in the typical experiment by Malaviya et al. [1972], the neutron source was a 60 MeV LINAC, and an evacuated neutron flight tube of length 28 to 100 m was needed to obtain adequate energy resolution.

The second type of experiment is exemplified by that of Gozani and d'Oultrement [1968], who measured the time-dependent reaction rate of a fission detector in a pulsed assembly. This type of experiment has the merits of requiring relatively simple apparatus and of preserving the time information. One important benefit of measuring the time response is that minor changes in the source energy distribution have virtually no effect after a few nanoseconds. The measurement is, therefore, much less sensitive to uncertainties in the source spectrum than is the stationary spectrum measurement. However, the differential energy spectrum information is lost.

With the advent of organic scintillator neutron spectrometers, it became feasible to measure both time and energy spectra. The penalty for gaining simultaneous time and energy information is a considerable increase in complexity of the data collection system and analytic procedures. For example, great care is needed to avoid systematic errors in the pulse height spectra due to the rapid change of the flux with time, and to reject the gamma rays to which the spectrometer is sensitive. Even after using pulse shape discrimination, it is not easy to be sure that systematic errors from gamma rays are eliminated.

Perhaps because of these difficulties, the technique of time-dependent neutron spectroscopy has not been widely used for evaluation of neutron data for fast reactor materials in simple assemblies. Deconninck and Monseu [1972] made some measurements on carbon, aluminium, iron and lead cubes with rather poor timing resolution and without the benefit of advanced spectrum unfolding codes. Pieroni [1974] made the first such experiment on a natural uranium assembly. This was an excellent pioneering experiment in which the whole process of time-dependent spectrum measurement and cross section adjustment was shown to be feasible.

Pieroni's results demonstrated one of the more serious problems with integral experiments. The cross section set which gives best agreement with a given experiment may not be unique. Thus both the Pieroni corrected data set and the KFKINR set [Keifhaber 1972] give better agreement with fast critical

assembly experiments than the KEDAK set from which they started, but each set is different (Figure 1). If the adjustment procedure were to lead to a genuine improvement in both cases, it would be accepted that the KFKINR set would be quite different from the original KEDAK set, as would the Pieroni's adjusted set. However, the KFKINR set would have to be substantially closer to Peironi's set than to the KEDAK set. This was not the case.

To compare the three data sets, the group-averaged sets presented by Pieroni were used. The percentage differences between the groups were squared and averaged, producing an r.m.s. percentage deviation between the sets. The r.m.s. percentage deviation of the KFKINR and the Pieroni sets from the KEDAK set were 7.5 and 10.1 per cent respectively. In the comparison of the KFKINR and Peironi sets, the value was 10.7 per cent. This is inconsistent with both the adjusted sets being closer to the truth than KEDAK. Clearly, several experiments carried out in different ways are required to resolve the inconsistency in reults.

2. EXPERIMENTAL DESIGN

The present work, in its conceptual phase when the Pieroni experiment was reported, benefits from a much deeper study of systematic errors of the technique. The following examples are representative. Firstly, the neutron source was chosen with an energy range within the dynamic range of the detector. This avoided having to subtract counts due to an estimated high energy component. Secondly, the monoenergetic responses were measured and tested to guarantee that the neutron spectroscopy system was self-consistent [Whittlestone 1980a]. The third systematic error to be examined in detail was timing walk. Measurements indicated that fast changing spectra can be severely distorted by a timing walk much smaller than the overall experimental timing resolution. A digital timing walk correction system was developed which virtually eliminated errors due to timing walk [Cawley and Whittlestone 1980]. Finally, the effect of pulse pile-up was found to be a significant source of error even when the probability of a count per beam pulse was as low as 0.02. In the present work, the errors range up to 7 per cent [Whittlestone 1980b].

A design study for the present experiment produced three strong indications that the detector should be placed inside the stack. First, it was clear that timing and high energy information would be lost as the

detection position moved from the centre to the external face. Since the scattering mean free path was approximately 5 cm, the proportion of neutrons which had undergone only one or two scatters would be very small at the stack surface. Thus the sensitivity of the experiment to cross section data in the 2 to 6 MeV range would probably be much greater inside the stack. Secondly, calculation of the system response would be easier. Within a few centimetres of the target, the flux would be nearly cylindrically symmetric. Not only would a Monte Carlo calculation be more efficient when the detector was inside the stack, but also there was the possibility of using a diffusion code for sensitivity studies. Thirdly, the background count rate of spontaneous gamma rays from the natural radioactivity of the stack could be reduced for a given neutron count rate. This was particularly important for any measurement in thorium. Although the spontaneous gamma ray count was only slightly influenced by the detector position, the neutron count rate would be about a factor of 10 higher at 6 cm from the target than at the surface [Moo 1973].

To enable the detector to be placed in the stack, a small NE213 scintillation detector (Nuclear Enterprises Ltd, Edinburgh, UK) was developed (Figure 2) which can slide into a 2.5 cm square hole in the uranium stack [Whittlestone 1980a].

Section 3 briefly describes the uranium assembly and the neutron source. The rather extensive measurements required to determine the neutron source conditions involved material not directly related to the spectrum measurements; this information has been published elsewhere [Whittlestone 1977a].

For the neutron spectrum measurements, it was necessary to ensure that, throughout the experiment, the basic calibrations of the time and energy scales were within known bounds. Section 4 begins with a description of the calibration and monitoring system, and finishes with details of the spectrum measurement. The effect of some instrumental instabilities is also assessed.

Section 5 presents the results of the spectrum measurement and a Monte Carlo calculation using the ENDF/B-IV data file. Some preliminary comparisons are made between the experiment and the calculation, and the relationship between the present experiment and some fission detector time spectra is discussed.

3. THE EXPERIMENTAL FACILITY

Details of the experimental hardware have been published elsewhere [Whittlestone 1977a]. The present discussion of the neutron source and the uranium assembly is limited to the details essential to an understanding of the time-dependent energy spectrum measurements (TDESM).

3.1 The Neutron Source

The neutron source for the TDESM was obtained from a beryllium target bombarded by a charged particle beam from a 3 MV Van de Graaff accelerator and mounted well away from extraneous neutron scattering materials. The accelerator performance and the elevated target station are described elsewhere [Whittlestone 1977a]. Essentially, the system delivered a pulse of about 3 ns FWHM, with a residual beam current less than 10^{-4} times the peak current. The number of neutrons scattered back to the detector from walls and fixtures was negligible.

Beryllium was chosen as the target material because it has the unique property of reacting with deuterons below 3 MeV in energy to produce copious quantities of neutrons with a range of energies up to about 7 MeV. Details of the neutron angle-dependent energy spectra are given by Whittlestone [1976, 1977b]. A deuteron energy of 2.3 MeV was chosen for the TDESM because the yield per microampere was adequate and the neutron energy spectrum was suitable (ranging up to 6.4 MeV). Also there was a reasonable probability of the accelerator achieving this energy on any given day.

3.2 The Uranium Assembly

The uranium assembly was a 406 mm cube composed of 512 precisely machined blocks. Some blocks were modified to form holes to accommodate the beryllium target at the centre of the cube and permit insertion of the detector. The assembly was supported on a table having a mild steel top with milled slots, to reduce neutron scattering, and three adjustable legs. The main features of the uranium assembly, the target and the table, are shown in Figure 3. The chemical composition of the blocks is given in Table 1.

4. MEASUREMENT OF TIME-DEPENDENT NEUTRON ENERGY SPECTRA

4.1 Introduction

During the experiment, the most important and unstable parameters were continuously monitored. The linear amplifier system gain was measured by a test pulser. Throughout the experiment, any changes of beam pulse shape or beam time pick-off were accounted for by viewing the target with a gamma ray detector and measuring the integrated beam pulse time profile. Drifts of the timing system were monitored by measuring both the beam pulse time profile and the neutron detector time spectrum with the same time-to-amplitude converter (TAC)/pulse height analyser (PHA) system. Where is was impracticable or unnecessary to provide continuous monitoring, calibrations were performed at appropriate intervals.

The basic functions of the electronics and calibration procedures are described in Sections 4.2 and 4.3, followed by a brief outline of the data collection system (Section 4.4) which was based on a PDP15 on-line computer. Finally, in Section 4.5, the measurement of the time-dependent spectra in the uranium stack is described and various errors are evaluated.

4.2 The Electronic System

The two basic functions of the electronics were:

(a) to amplify and shape the linear pulse from the photomultiplier for analysis by the computer; and

(b) to provide a timing signal with each pulse.

Thus each event could be stored in a different region of the computer according to the time of the event in relation to the accelerator beam pulse. Additional circuits were required to 'veto' gamma ray events and to perform basic calibrations. Still more circuits were necessary to monitor the prevailing instability of all other devices. The final system to carry out all these functions is represented schematically in Figure 4.

The beam pick-off pulse passed through a complex logic circuit before it reached the TAC stop input. This circuitry ensured that only the gamma detector pulses were recorded in the first 50 ns of the TAC sweep and only

scintillator probe events in the final 150 ns, producing the time spectrum sketched in the computer box of Figure 4. Another subtlety was the processing of the trigger signal from the precision pulse generator (PPG). To be recorded in the pulse height spectrum, the pulse in the linear system had to be accompanied by three other pulses, as if it were a real detector pulse. Two of these extra pulses indicated a 'neutron' event and a valid timing event. The third was a pulse fed through the summing amplifier into the analog-to-digital converter (ADC) which processed the timing events from the TAC. A pseudo timing event was therefore recorded in the time spectrum. The test pulse in the linear system then appeared in the pulse height spectrum of a time window embracing the pseudo time event.

4.3 Calibrations

Seven calibrations were required for day-to-day operation of the experiment. Amplifier gain monitoring and measurement of the beam pulse time profile have already been discussed adequately. A third set the pulse shape analyser ratio to reject 98 per cent of the counts from a ^{137}Cs source. A fourth established the pulse height scale in $\underline{H}_e$* (1 $\underline{H}_e$ is the pulse height from a 1 MeV electron in the scintillator). This was done by adjusting the precision pulse generator to the half height of the Compton edge of the ^{137}Cs reference source. The half height was at 0.4964 $\underline{H}_e$ = Compton edge energy x 1.04 [Flynn et al. 1964]. By setting the pulser to other positions, the zero channel and linearity were determined.

The remaining three calibrations refer to timing. The absolute timing of the probe time scale was established by placing the scintillator probe to view the target directly and count the gamma rays. A peak of the same shape as the gamma monitor peak appeared in the right hand portion of the time spectrum (Figure 4). After correction for the gamma ray flight time, the relationship between the monitor peak and the absolute timing of the probe spectrum is known.

In the next timing calibration, the number of channels between the gamma detector peak and the half height of the leading edge of the probe neutron time spectrum was monitored from run to run. This provided a check on the accuracy of the absolute timing (see Section 4.5).

* The $\underline{H}_e$ is identical to 'MeVe' used elsewhere (cf. Whittlestone 1980d], and accords with AAEC practice in choice of notation.

Finally, the time scale of the time spectrum was measured using the accurate 100 ns delay increments from a digital delay based on a 10 MHz crystal. Measurements were made of the number of channels between, say, 10 and 110 ns and 50 and 150 ns. The mean was taken as the calibration and the difference as an index of non-linearity.

4.4 The Experimental Data Collection System

The PDP15 computer was equipped with a CAMAC crate incorporating scalers and three ADCs, with a machine language dual parameter program, DIGWIN-W, and a FOCAL higher level language [DEC 1969] to control CAMAC and input/output functions. A FOCAL program was written to facilitate operation of the experiment. Apart from timing or writing messages about the state of the experiment at preset counts, this program made it possible to work in units of nanoseconds for timing and $\underline{H}_e$ for pulse heights. Thus, digital windows and timing walk were entered in nanosecond units using a conversational style of programming which minimised operator errors. A listing of the program is given in Appendix A.

4.5 The Spectrum Measurement

The experiment was run over four days during which time six nominally identical sets of data were accumulated; every calibration varied throughout this period. The discussion will proceed from the easier to the more difficult aspects of these variations. At the end of this section, the standardisation and summation of the data will be discussed. A summary of the physically important data for the summed spectra is given in Table 2.

Changes in the pulse height scale were insignificant during any one run (approximately 0.3 per cent) and of no significance between runs because of the subsequent standardisation. Nor was there any problem with the pulse shape analyser, no adjustments being required during the four days.

Accelerator stability was more of a problem because the pulse width gradually increased from 2.4 to 5.0 ns FWHM, while the count rate fluctuated between 2000 and 11 000 counts s^{-1}, with an average of about 8000 counts s^{-1}. The pulse width variations were more of a hindrance than a source of error, because the continuous monitoring of the beam pulse kept track of any timing shifts during the measurement. Sufficient reproducibility of timing was obtained by adjusting the time windows at the start of each run. However, the

count rate fluctuations prevented a meaningful evaluation of pulse pile-up effects [Whittlestone 1980a].

Using the formalism developed by Whittlestone [1980a], the increase in counts recorded because of pile-up at a count rate of 11 000 counts s^{-1} was shown to vary by a few per cent over each pulse height spectrum (Figure 5). Had the count rate during the experiment been constant, the spectra could have been corrected. In the present experiment, the time history of the count rate was not recorded, and so the pile-up contribution could not be calculated. It was only possible to regard the pile-up at a count rate of 11 000 counts s^{-1} as an upper limit and treat it as an error. For the relatively smooth spectra in the uranium stack, with their fairly high proportion of low energy neutrons, errors in the pulse height spectra translated into similar errors in the unfolded energy spectrum.

The worst problem encountered during the experiment was drifting of the TAC, with variations of ± 0.7 per cent from the mean of 0.0719 ns per channel. Although this represented only 0.5 ns over the 77 ns time range of the neutron spectrum, it introduced a 1 ns error into the absolute timing determination, which was based on the relative position of time reference points situated 150 ns apart. An error of 1 ns in the timing of the first time window at about 3 ns after the beam pulse was unacceptable. Fortunately, a Monte Carlo calculation [Rainbow and Whittlestone 1980] of the neutron energy spectra and time response of the experiment has been made, showing, among other things, that the response of the uranium stack to an impulse at the target is extremely fast. In fact, the count rate as a function of time reached its maximum within one 0.1 ns time channel. This meant that the leading edge of the calculated time response with the beam pulse timing folded in was very close to the integral of the beam pulse. Thus the absolute timing of the experimental beam pulse could be determined from the neutron detector time response. To illustrate this, a calculation of the detector response was made for an impulse and the experimental beam pulse shape. When the timing of the impulse was matched to the peak of the true beam pulse, the half height of the beam pulse broadened response was exactly at the leading edge of the impulse response (Figure 6).

The first step in the experimental analysis was to add all the data together. The pulse height spectra were first standardised to channel 1 = 0, channel 512 = 3.5 $\underline{H}_e$, using the AND code [Whittlestone 1980b], then added, doing a χ^2 test which showed that all the data at later times were

consistent, but inconsistent at early times. This was expected in view of the different beam pulse shapes and times. Figure 7 gives a representative sample of the beam pulse time profiles, adjusted to a time zero 8.9 ns before the start of the first time window. These adjusted beam pulse time profiles were added together to produce the profile which would have produced the summed time-gated pulse height spectra, had the accelerator produced that profile steadily for four days and the TAC not drifted.

The standardised summed pulse height spectra were analysed using the code UNF [Whittlestone 1980b].

5. RESULTS AND DISCUSSION

5.1 Results

Table 2 contains a specification of the time-dependent neutron energy spectrum measurement, including the overall accuracy, timing, amplitude and neutron energy resolutions, and the time boundaries of the windows from which the neutron spectra were taken. It may be noted that the accuracy of the energy spectra is quoted as 10 per cent plus statistical errors plus oscillations. These oscillations are artifacts of the unfolding process and represent local perturbations from the true solution. One way to mitigate the effects of oscillations in a spectrum having no fine structure is to regroup the spectrum energies into wider energy groups. The aim in selecting the new groups was to eliminate structure which was not credible from the solution, while keeping the groups as narrow as possible. Table 3 gives the new group boundaries. The original and regrouped neutron energy spectra from the window at 12 ns are shown in Figure 8a. It is believed that the amplitude of the oscillations has been reduced to less than the 10 per cent systematic error on the spectra owing to other factors.

The Monte Carlo calculations [Rainbow and Whittlestone 1980] for the 12 ns window are shown in Figure 8b, with its original groups and those defined in Table 3. Evidently, there is no serious loss of information resulting from the broadening of the energy resolution of the results. The benefit of improved statistical accuracy in the higher energy groups at later times far outweighs any loss.

Figures 9 to 11 show the neutron energy spectra derived from experiment and calculation using the ENDF/B-IV cross section set. These results are tabulated in Appendix B. The curves have been normalised by the factor which makes the experiment and theory match at 2.75 MeV in the 21 ns time window. The pairs of lines give the calculated values plus and minus the statistical error. As a basis for discussion, a fission neutron spectrum is superimposed on the spectra at 16 ns. Details of the Monte Carlo calculation are given by Rainbow and Whittlestone [1980]. Briefly, the detector geometry and material cross sections were included explicitly. Fifty energy groups were used, spanning the range 10 keV to 10 MeV. Perturbations from the iron table on which the stack rested proved to be negligible. The only significant systematic error in the calculation arose from errors in the uranium cross sections.

5.2 Comparison of Experiment with Calculation and Fission Spectrum

The objective of the experiment has been realised by the presentation of the results in the previous section. However, a few immediate comparisons with theory are possible. The first impression from the results (Figures 9 to 11) is that there is quite good agreement between experiment and theory after 12 ns. During the first 1.9 ns, the calculation predicts too 'hard' a spectrum, but the prediction changes faster than the experiment, and by 5.9 ns is too 'soft', the discrepancy diminishing at later times.

To put these impressions on a more quantitative basis, the comparison was split into considerations of integral time response, which will be discussed in the next section, and spectrum shape. The difference between the experimental and theoretical spectrum shapes was expressed as the variance $x^2/(N-1)$, minimised by applying a scale factor to the theoretical spectrum at each time (Figure 12). Allowance was made for the 10 per cent systematic error from efficiency and pile-up. The experimental and theoretical energy spectra did not have the same shape at any time, although at time windows between 16 and 29.5 ns, the variances were very close to 2, the value for 5 per cent probability of agreement.

The next step was to look for agreement between parts of the spectra. It was clear from the calculation that a high proportion of the high energy counts at later times were due to fission neutrons. As a matter of interest, the fission spectrum from ^{238}U was scaled to match the measured and calculated spectra above various energies. The later the time, the lower was the energy

beyond which the fission spectrum was a good match (Figure 13). The criterion for matching was a x^2 probability of > 5 per cent.

Considerations such as these, together with group time responses will provide part of the basis for adjusting the cross sections to obtain better agreement between experiment and theory. At a more basic level, it was reassuring that the experiment agreed with the theory when the theory predicted a fission spectrum. Intuitively, it would seem that only unbelievable errors in the sections could cause disagreement in these cases. Thus the observed agreement with the fission spectrum gave confidence in the accuracy of the regrouped energy spectra.

5.3 Comparison with Fission Detector Measurements

An adjunct to the measurement of time-dependent neutron energy spectra was the measurement of detector count rate as a function of time after the beam pulse. A measurement of similar time spectra in the same uranium stack with the same source has been made by Rainbow [1980] using ^{237}Np and ^{235}U fission detectors. The relative efficiencies of the ^{235}U, ^{237}Np and NE213 detectors as a function of energy exhibit detection thresholds at 0, 0.6 and 0.8 MeV respectively (Figure 14a). Since most of the neutrons have energies below 1 MeV after 12 ns (Figure 9), the decay rates will be very sensitive to errors in the cross sections in just the region where the detector efficiencies are most different. When the experiment and theory for the time responses of these detectors are compared (Figure 14b), the ^{235}U decay rate prediction is too low, that for ^{237}Np about right and that for the NE213 detector too high. Thus, using a very crude two-group model, it would appear that the calculation for energies below 0.8 MeV gives too low a decay rate whereas the converse applies for energies above 0.8 MeV. The agreement with the ^{237}Np detector would seem to be a consequence of the cancellation of a number of errors.

Two conclusions may be drawn from this. Firstly, it would be worth attempting to push the energy threshold of the NE213 spectrometer down as far as possible to investigate problems with the inelastic cross sections in the sub-MeV range. Secondly, use of the NE213 detector as a threshold detector has already indicated problems with the inelastic cross sections which dominate the time response above 1 MeV [Pieroni 1974]. A thorough analysis of the energy spectrum data from the NE213 detector should lead to some very well informed guesses at changes which should be made in these cross sections.

6. CONCLUSIONS

A set of time-dependent neutron energy spectra in a pulsed uranium assembly has been measured with sufficient accuracy to show that there are significant discrepancies from a Monte Carlo calculation. Current indications are that these discrepancies are due to inaccuracies in the inelastic cross section data for ^{238}U [Corcuera 1975; Bluhm et al. 1974]. The present experiment has provided a basis for correction of these cross sections.

In addition, the original concept of the experiment has been vindicated. Both the detector positioning and measurement of time-dependence of the spectra have given valuable insight into the behaviour of the neutrons in the assembly. By placing the detector inside the stack, perturbations by scattering from external hardware were virtually eliminated and the Monte Carlo calculation was more efficient. This was because the flux was higher and the detector could be modelled by a cylinder around the beam axis [Rainbow and Whittlestone 1980]. But most importantly, it was possible to observe the extremely rapid softening of the neutron energy spectrum from a predominantly 5 MeV spectrum 1.9 ns after the beam pulse to a spectrum with only a few per cent of neutrons above 2 MeV by 8 ns. During this time, the spectrum was most sensitive to the inelastic cross sections between 2 and 6 MeV. Since the experiment with the detector inside the stack was only just able to follow the spectrum changes, it is clear that a detector on the surface would have had substantially less chance of providing significant data in this energy region. Also, the value of measuring time-dependence is nicely demonstrated by the change in the calculated spectra from too hard to too soft during the first 8 ns. A stationary experiment could not have detected such a change. It is anticipated that the sensitivity studies to be carried out on this experiment will more rigorously justify the effort of measuring simultaneous time and energy dependence.

Comparison of time spectra from the present measurement with time spectra from two detectors with lower energy thresholds has indicated that there are significant cross section discrepancies at energies below 1 MeV. Thus it would be desirable to measure energy spectra down to about 0.2 MeV.

7. ACKNOWLEDGEMENTS

Many members of the AAEC Physics Division have assisted in this work. I am indebted to Mr W. Gemmell for his support. Thanks are due particularly to Drs A.I.M. Ritchie, D. Lang and B.E. Clancy for valuable discussions. Messrs A. Van Heugten, J. Fallon and H. Broe helped to keep the accelerator operational and Mr D. Stevenson assisted in the construction of the detector system. Messrs R.J. Cawley and M.D. Scott provided assistance with the on-line computer, and the help of Mr G.D. Trimble with FORTRAN programming and Mr E. Clayton with detector calculations was invaluable. Finally, I wish to thank Mr D. Stathers for constructing the glass scintillation chambers and Mr H. Wyllie for providing the gamma ray and electron calibration sources.

8. REFERENCES

Bluhm, H., Feig, G and Werle, H. [1974] - Nucl. Sci. Eng., 54:300.

Cawley, R.J. and Whittlestone, S. [1980] - Digital timing walk correction and its application to a time-dependent fast neutron energy spectrum measurement. Submitted to Nucl. Instrum. Methods.

Corcuera, R.P. [1975] - Nucl. Sci. Eng., 58:278.

DEC [1969] - PDP15 Systems Focal Programming Manual. Digital Equipment Corp., Maynard, Mass. DEC-15-KJ2A-D.

Deconninck, G. and Monseu, P. [1972] - J. Nucl. Energy, 26:537.

Flynn, K.F., Glendenin, L.E., Steinberg, E.P. and Wright, P.M. [1964] - Nucl. Instrum. Methods, 27:13.

Gozani, T. and d'Oultremont, P. [1968] - GA-8536.

Greebler, P., Hutchins, G.A. and Cowan, C.L. [1970] - IAEA-CN-26/102, p.17.

Kabir, S.M. and Cooper, P.M. [1972] - J. Nucl. Energy, 26:573.

Keifhaber, E. [1972] - KFK-1572.

Malaviya, B.K., Kaasal, N.N., Bocker, M., Burns, E.T., Ginsberg, A. and Gaerttner, E.L. [1972] - Nucl. Sci. Eng., 47:329.

Moo, S.P. [1973] - Pulsed neutron experiments on thorium. Ph.D. thesis, University of Tasmania.

Pieroni, N. [1974] - KFK-1968.

Ragan, C.E. III, Auchampaugh, G.F., Hemmendinger, A. and Silbert, M.G. [1976] - Nucl. Sci. Eng., 61:33.

Rainbow, M.T. [1980] - AAEC report in preparation.

Rainbow, M.T. and Whittlestone, S. [1980] - Time dependent fast neutron energy spectra in a depleted uranium assembly. In preparation for submission to a a journal.

Whittlestone, S. [1976] - AAEC/E399.

Whittlestone, S. [1977a] - AAEC/E420.

Whittlestone, S. [1977b] - J. Phys. D., Appl. Phys. 10:1715.

Whittlestone, S. [1980a] - AAEC/E484.

Whittlestone, S. [1980b] - AAEC/E489.

Whittlestone, S. [1980c] - The effect of pulse pile-up on discrimination between neutrons and gamma rays. Submitted to Nucl. Instrum. Methods.

Whittlestone, S. [1980d] - Nucl. Instrum. Methods, 169:215.

TABLE 1
COMPOSITION OF DEPLETED URANIUM BLOCKS

Element	Analysis $\mu g\ g^{-1}$	Element	Analysis $\mu g\ g^{-1}$
C	141	Cu	20
Cd	< 0.1	Hg	< 1.4
B	< 0.2	Li	< 1.0
Fe	85	Ag	< 0.1
Mn	30	V	< 5
Ni	29	Mo	4
N	32	Mg	< 2
Al	70	Th	< 2
Si	90	^{235}U	0.20
Cr	< 3	^{238}U	99.7

TABLE 2

SPECIFICATION OF THE TIME-DEPENDENT NEUTRON ENERGY SPECTRUM MEASUREMENT

Electronic System	
Pulse height range	0.1 to 3.5 MeVe
Resolution	0.00685 MeVe/channel
Accuracy	±0.4%
Neutron source	Neutron energies in the range 0 to 6.4 MeV from the $^{9}Be(d,n)^{10}B$ reaction in a thick Be target bombarded by 2.3 MeV deuterons (Whittlestone 1976).
Timing:	
Resolution	Time spectrum channel width 0.072 ns. Beam pulse approximately Gaussian, width 3.0 ns FWHM.
Walk	±0.1 ns after active walk correction
Accuracy	±0.7%
Unfolded Neutron Energy Spectra	
Neutron energy range	0.6 to 6.4 MeV
Resolution	20% based on results shown in Figure 5-4. Initial analysis in 0.1 MeV groups.
Energy spectrum accuracy	10% from pile-up effects and efficiency errors in addition to statistical errors and oscillations arising from the unfolding process.
Time: Range	0.9 to 82 ns after the peak of the beam pulse.

Window No.	1	2	3	4	5	6	7	8	9	10	11	12	13	14	15	16	17
*Upper bound	2.9	4.9	6.8	9.0	11	13	15	17	22	27	32	37	42.2	52.2	62.2	72.2	82.2
*Average time	1.9	3.9	5.9	7.9	10	12	14	16	21	26	29.5	34.5	39.6	47.2	57.2	67.2	77.2

*Relative to peak of beam pulse, ns

TABLE 3

ENERGY BOUNDARIFS FOR REGROUPED NEUTRON ENERGY SPECTRA

Group No.	Boundary (MeV)	Centre (MeV)
	0.6	
1		0.8
	1.0	
2		1.25
	1.5	
3		1.75
	2.0	
4		2.25
	2.5	
5		2.75
	3.0	
6		3.25
	3.5	
7		4.0
	4.5	
8		5.0
	5.5	
9		5.95
	6.4	

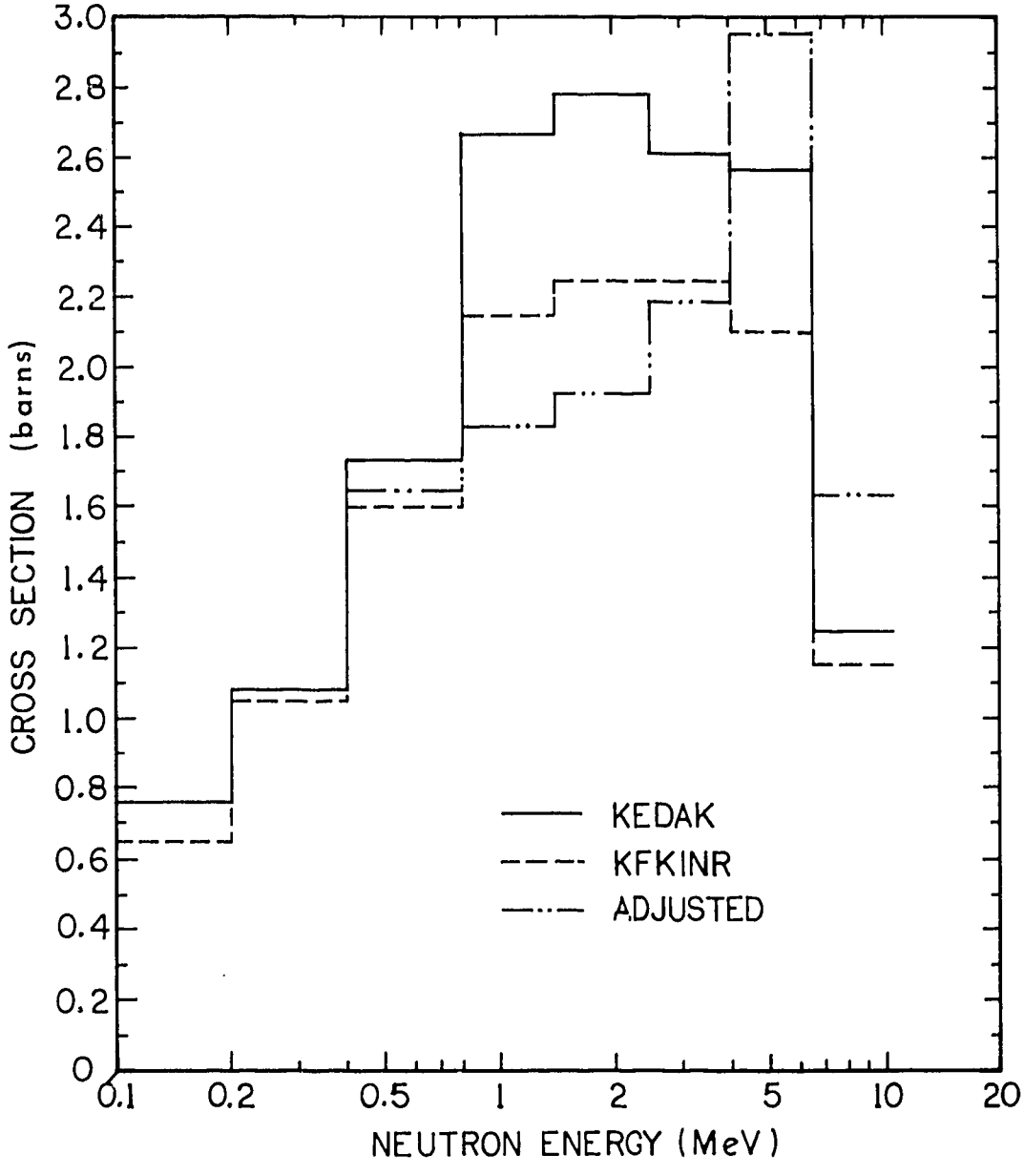

FIGURE 1. GROUP INELASTIC SCATTERING CROSS SECTIONS FOR ^{235}U

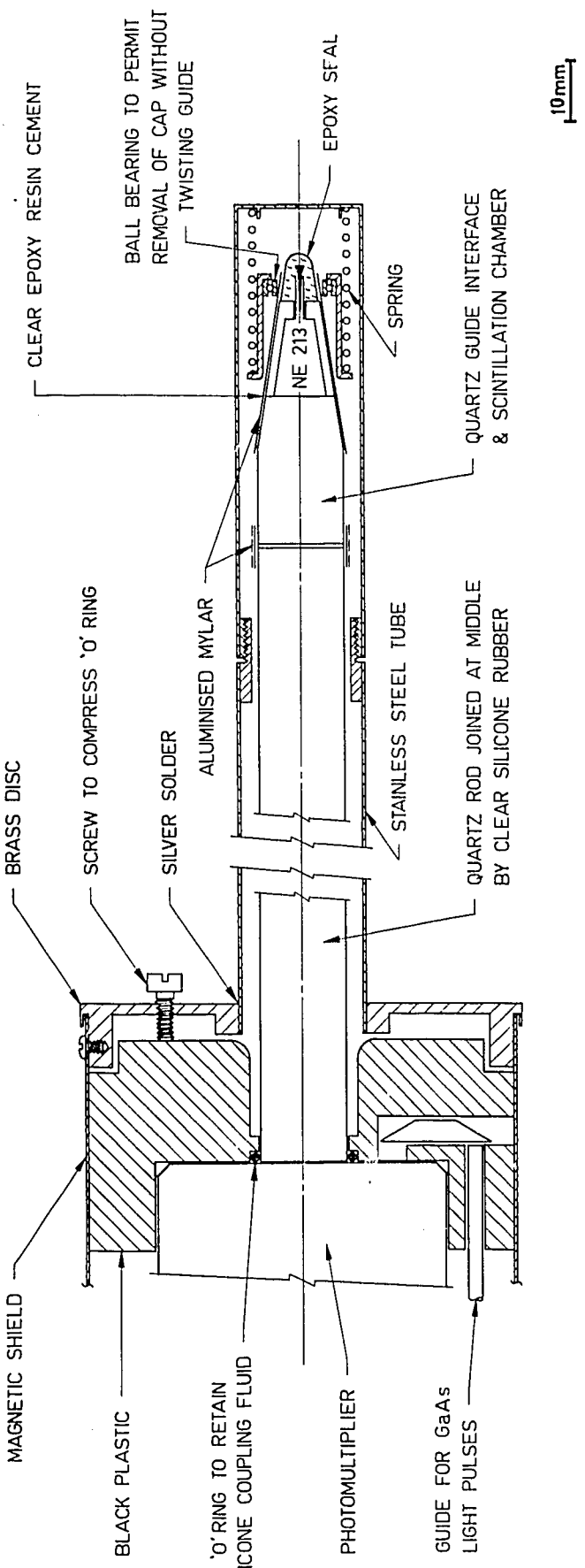

FIGURE 2. THE SCINTILLATOR PROBE

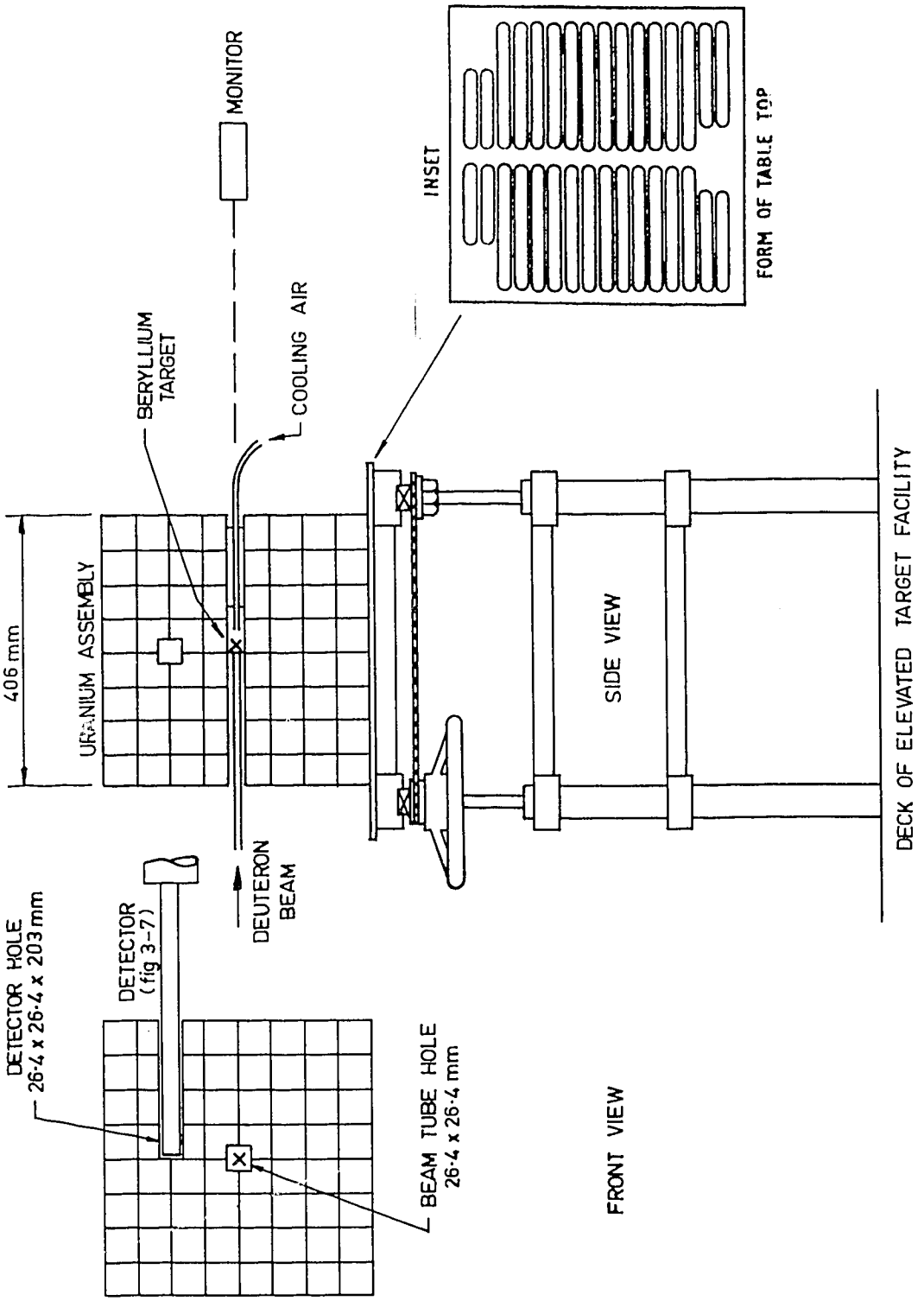

FIGURE 3. SCHEMATIC DIAGRAM OF THE URANIUM ASSEMBLY AND SOME ASSOCIATED FACILITIES

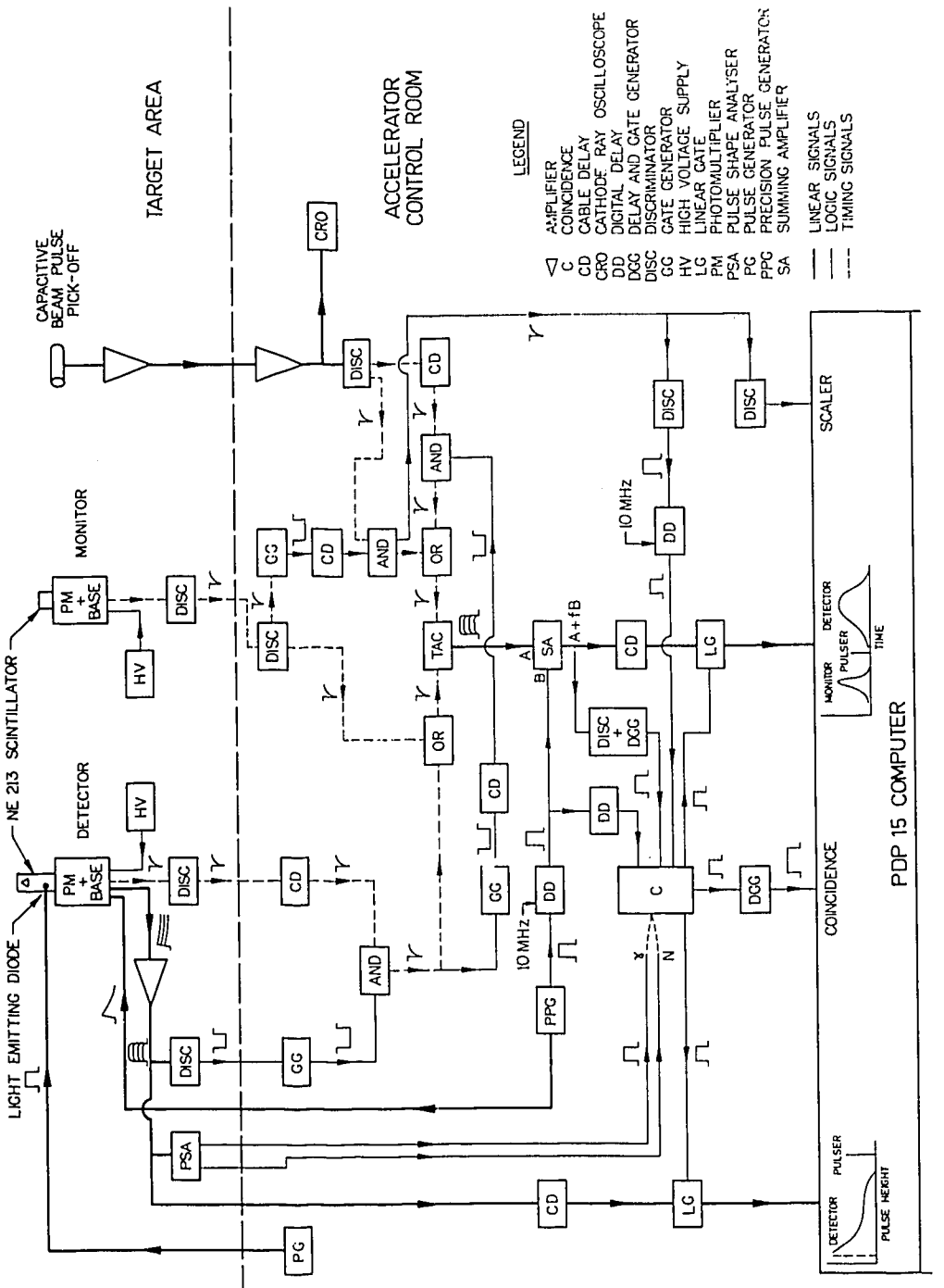

FIGURE 4. SCHEMATIC DIAGRAM OF THE TIME-DEPENDENT NEUTRON ENERGY SPECTRUM MEASUREMENT SYSTEM

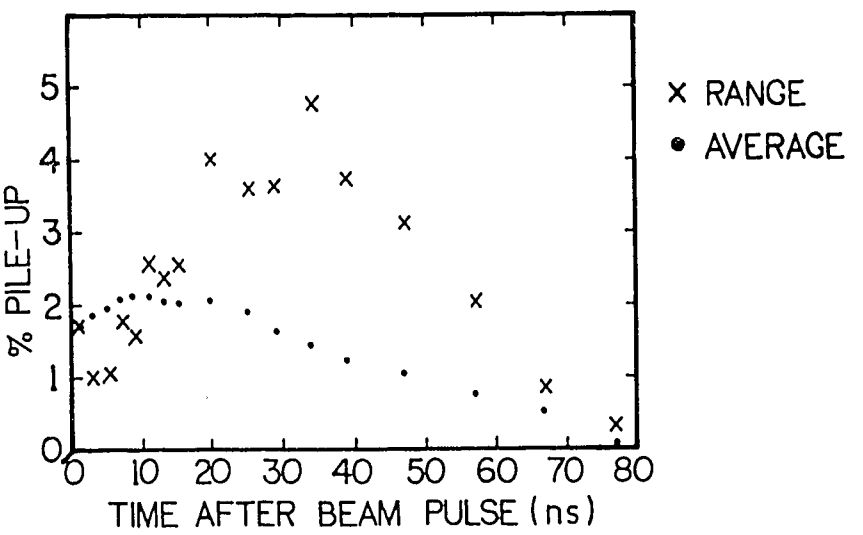

FIGURE 5. RANGE AND AVERAGE % PILE-UP VERSUS TIME AFTER BEAM PULSE

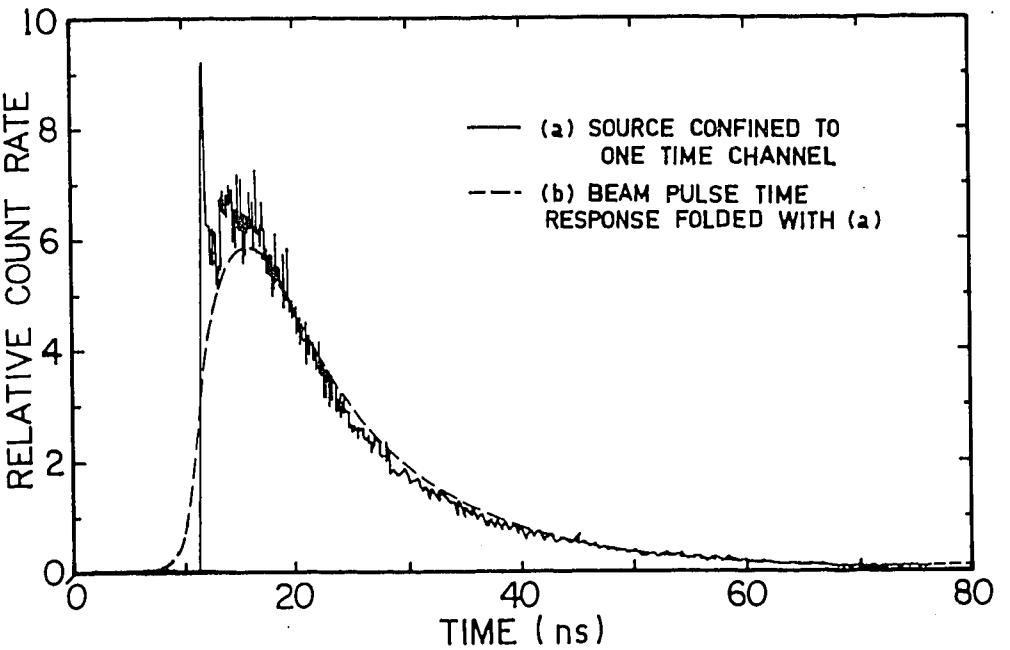

FIGURE 6. TIME RESPONSE OF SCINTILLATOR DETECTOR IN URANIUM STACK CALCULATED BY MONTE CARLO CODE

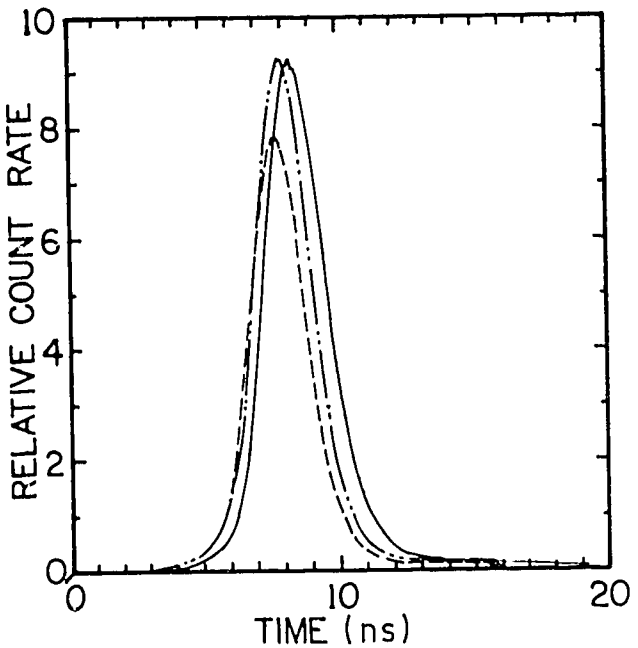

FIGURE 7. TYPICAL BEAM PULSE TIME RESPONSES.
TIME WINDOW 1 STARTS AT 8.9ns

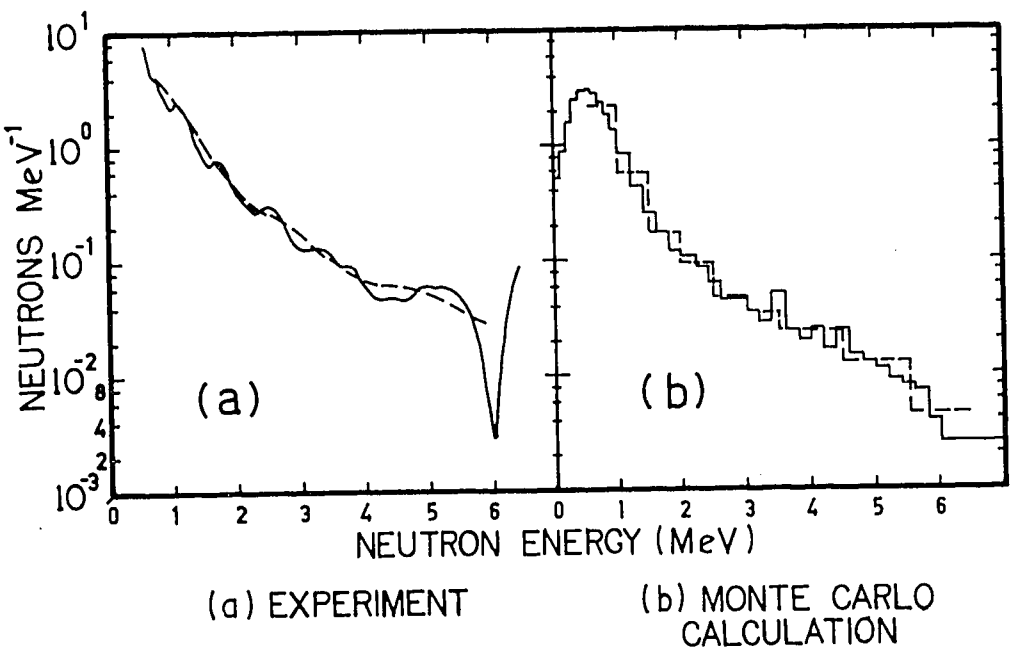

FIGURE 8. ORIGINAL AND REGROUPED NEUTRON ENERGY SPECTRA FROM TIME WINDOW AT 12ns

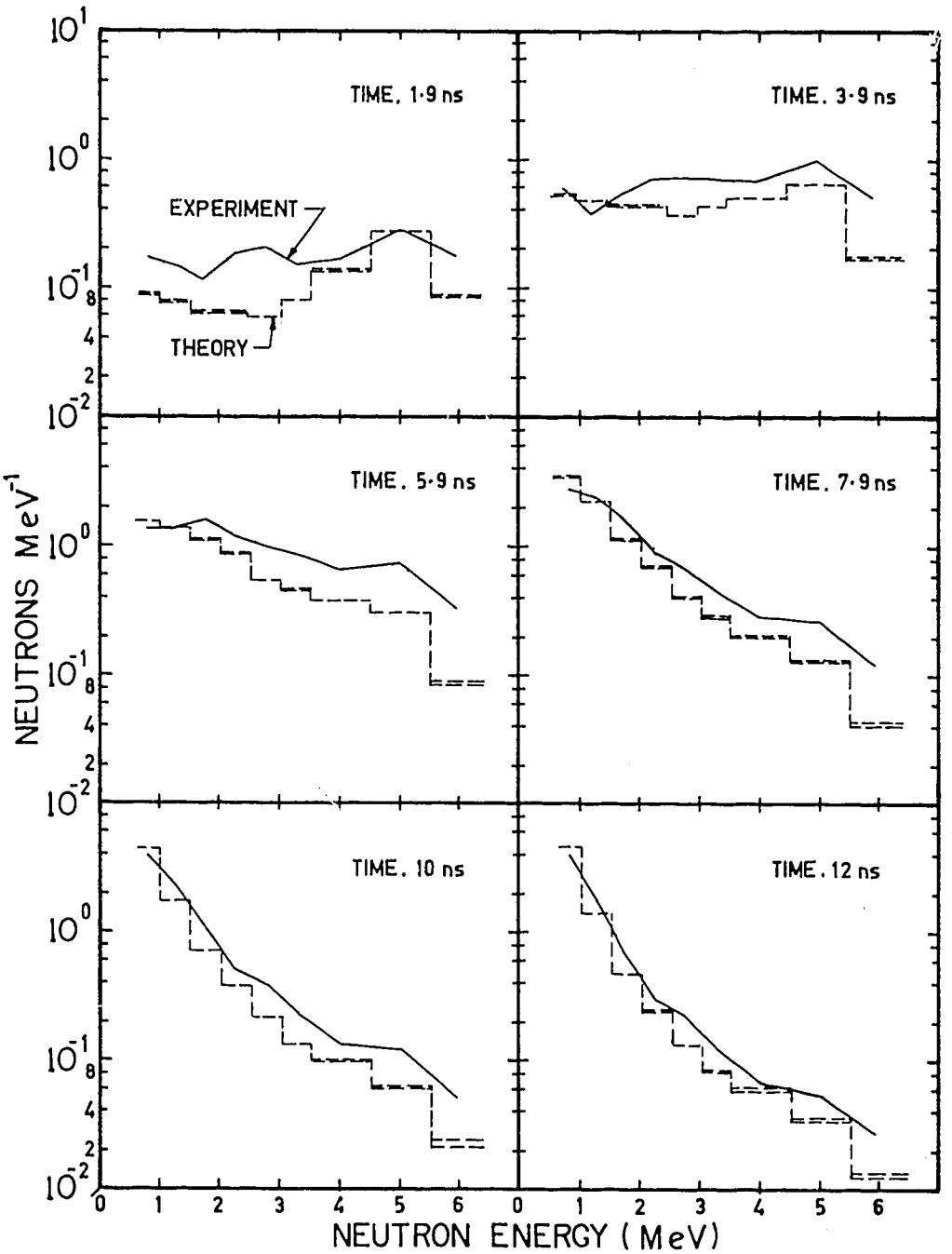

FIGURE 9. NEUTRON ENERGY SPECTRA IN URANIUM STACK 1.9 TO 12ns AFTER THE BEAM PULSE PEAK

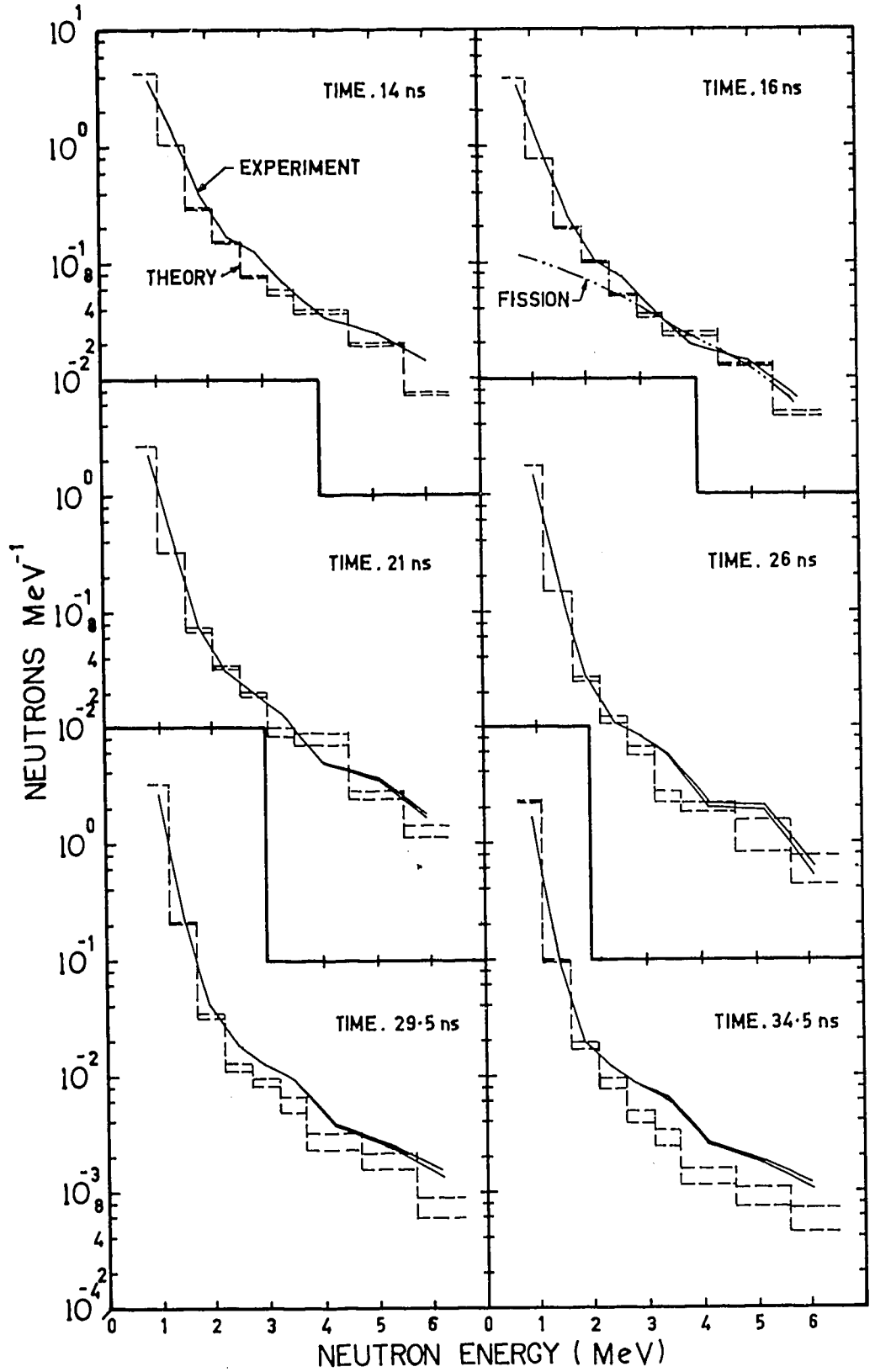

FIGURE 10. NEUTRON ENERGY SPECTRA IN URANIUM STACK 14 TO 34.5 ns AFTER THE BEAM PULSE PEAK

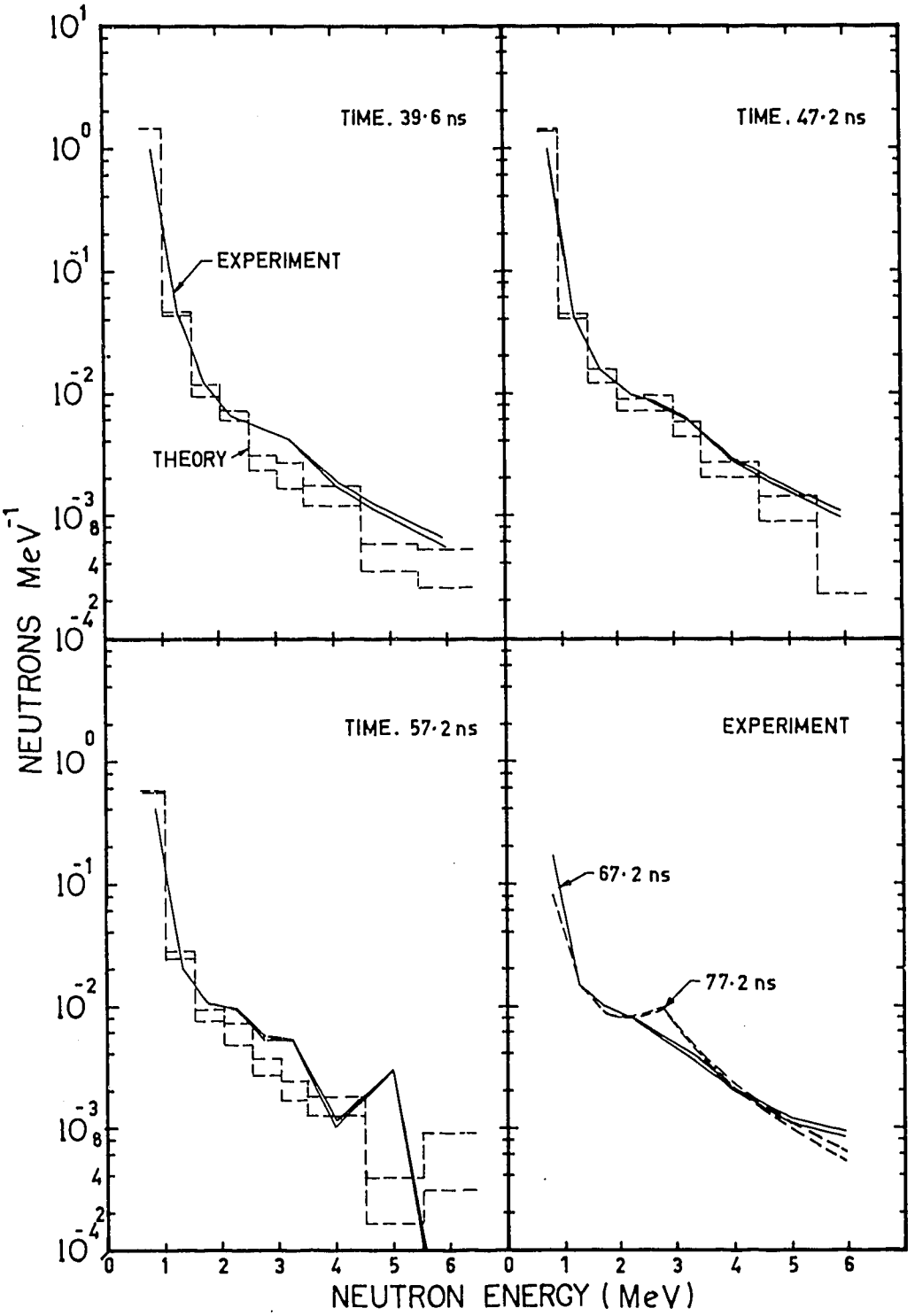

FIGURE 11. NEUTRON ENERGY SPECTRA IN URANIUM STACK 39.6 TO 77.2 ns AFTER THE BEAM PULSE PEAK

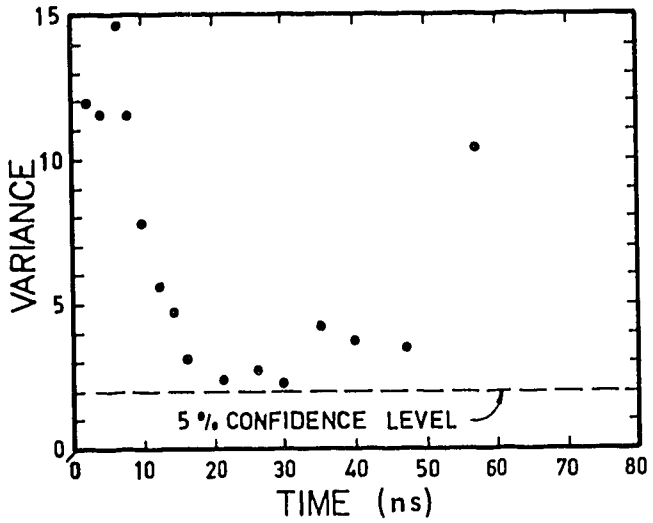

FIGURE 12. COMPARISON OF EXPERIMENTAL AND THEORETICAL NEUTRON ENERGY SPECTRUM SHAPES VERSUS TIME AFTER BEAM PULSE PEAK

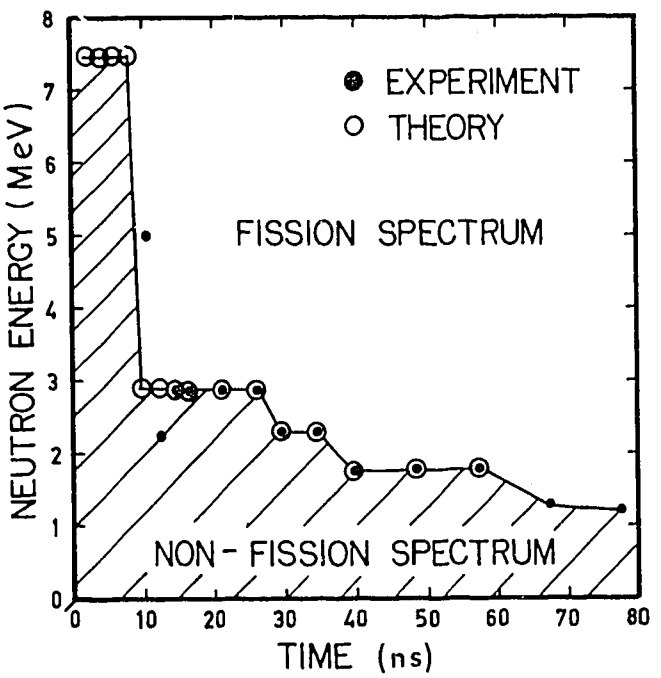

FIGURE 13. NEUTRON ENERGY ABOVE WHICH SPECTRUM MATCHES FISSION SPECTRUM VERSUS TIME AFTER BEAM PULSE PEAK

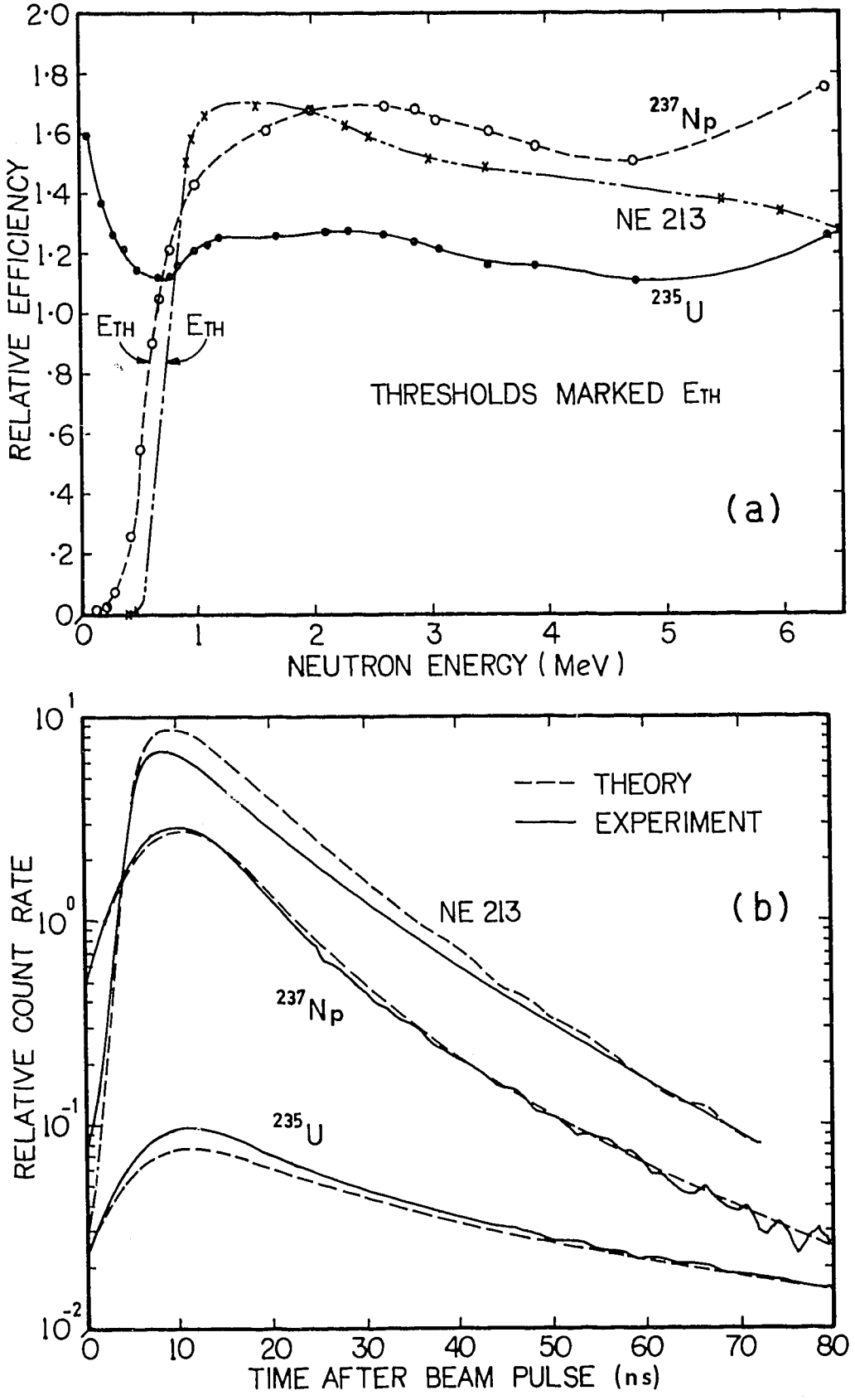

FIGURE 14. THE RELATIVE EFFICIENCIES (a) AND TIME SPECTRA (b) OF THREE DETECTORS . NORMALISATION OF ALL CURVES ARBITRARY

APPENDIX A

LISTING OF FOCAL PROGRAM 'WALK'

```
LIST WALK SWX

C PHA-F
01.02 COMMON C1,C2,AV,SM1,SM2,HALF,CZ,NL,SX,SY,SXY,SXX,M,B,NCAL,PH
01.03 COMMON (PHC,1,1,20),(CHC,1,1,3/20)
01.05 COMMON SC,TCAL,TZ,CH,EC1,EC2,CC1,CC2,ECF,CEZ,E,NS,NR
01.06 COMMON (CHT,1,1,20),(TS,1,1,20),G,NDW,W,WS,NW1,WT,WSS
01.07 COMMON (CW,1,1,22),(TT,1,1,22),TP,HMS,LMS
01.08 COMMON R1,R2,CM,NCH,NW,CP,PSC,CHP
01.10 ZWT;RUN 0;INC;F J=0,3;CAMAC 1,3,J,24
02.05 CAMAC 1,30,9,24;C     **************START DATA TAKING
03.05 T %10.00,!,"SCALERS  ";F J=0,3;CAMAC 1,3,J,0,SC;T SC,"    "
04.05 CAMAC 1,3,15,9;D 7.05;C ZERO SCALERS  , PRESET SCALER 0 ************
05.05 CAMAC 1,30,9,26;C STOP DATA TAKING
06.05 F J=0,NDW;Z J
07.05 CAMAC 1,3,0,16,CP;EXIT 1,3;CAMAC 1,3,0,26
10.01 C CALCULATE AND PRINT TIME AT 'CH' BEFORE CHANNEL TZ. SET CH
10.02 T !,"NS/CH ";A TCAL;T "  ZERO TIME CHANNEL ";A TZ;T "  CHANNEL ";A CH
10.03 T %10.03,"  TIME = ",(TZ-CH)*TCAL
10.04 S NCH=512
10.05 T !,"ENTER NUMBER OF CALIBRATION POINTS ";A NCAL
10.06 T !,"ENTER NCAL PAIRS OF CHANNEL, ENERGY ";F J=1,NCAL;A CHC(J),PHC(J)
10.07 T !,"ENTER PRESET COUNT ";A PSC;S CP=2↑24-PSC;D 7.05
10.08 T "0'FLOW CHANNEL ";A CHP
11.11 T !,"ENTER CHANNEL ";A CH;D 10.03
11.33 T !," ENTER TIME ";A CH;T %10.03," CHANNEL = ",TZ-CH/TCAL
12.05 T !,"ENTER CHANNEL ";A CH;S J=1;C  CALCULATE ENERGY *********
12.10 S J=J+1;IF (NCAL-J)14.05;IF (CHC(J)-CH)12.10,12.15,12.15
12.15 S K=J-1;T "  PULSE HEIGHT = ",%8.04
12.20 T PHC(K)+(CH-CHC(K))*(PHC(K)-PHC(J))/(CHC(K)-CHC(J))
13.05 T !,"ENTER PULSE HEIGHT ";A PH;S J=1;C CALCULATE EENERGY CHANNEL ****
13.10 S J=J+1;IF (NCAL-J)14.10;IF (PHC(J)-PH)13.10,13.15,13.15
13.15 S K=J-1;S CH=CHC(K)+(PH-PHC(K))*(CHC(K)-CHC(J))/(PHC(K)-PHC(J))
13.20 T %8.02,"  CHANNEL = ",CH
14.05 S J=NCAL;D 12.15;D 12.20
14.10 S J=NCAL;D 13.15;D 13.20
20.01 C WALK FUNCTION LOADING ROUTINE
20.02 C THE NUMBER OF CHANNELS WALK SHIFT FOR EACH CHANNEL BE LOADDED INTO
20.03 C THE WAK TABLE AND REGION NR.
20.04 C "D 21" REQUIRES WALK IN NS,PH IN CHANNELS
20.05 C "D 22" REQUIRES WALK IN NS,PH IN MEVE
20.20 S G=(TS(1)-TS(2))/(CHT(1)-CHT(2));S TS(1)=TS(1)-G*CHT(1);S CHT(1)=0
20.25 S G=(TS(NS)-TS(NS-1))/(CHT(NS)-CHT(NS-1))
20.26 S TS(NS)=TS(NS)+G*(NCH-CHT(NS));S CHT(NS)=NCH
20.31 F K=2,NS;S L=K-1;S G=(TS(K)-TS(L))/(CHT(K)-CHT(L));D 21
20.90 DON
21.05 F M=CHT(L),CHT(K);S T=(TS(K)+G*(M-CHT(K)))/TCAL+.5;WALK T,M;USET NR,M,T
22.05 T !,"ENTER NS,NR ";A NS,NR;Z NR
22.10 T !,"ENTER NS PAIRS OF E(MEVE),WALK (NS) "
22.15 F L=1,NS;A PH,TS(L);S J=1;D 13.10;S CHT(L)=CH
22.20 DOFF;D 20
23.05 T !," ENTER NS,NR ";A NS,NR;Z NR
23.10 T !," ENTER NS PAIRS OF CHT,TS(NS) "
23.15 F J=1,NS;A CHT(J),TS(J)
23.20 DOFF;D 20
30.01 C SET UP DIGITAL WINDOWS.
30.02 C NDW(NUMBER OF WINDOWS), W(WINDOW WIDTH - NS), WS(SPACING =  NS)
30.03 C NW1(FIRST WINDOW TO BE SET)
30.04 T !,"ENTER NDW ";A NDW;T "  WIDTH NS ";A W;T "  SPACING ";A WS
30.05 T "  FIRST WINDOW ";A NW1
```

(Continued)

```
30.10 S WT=FITR(W/TCAL);S WSS=W+WS
30.15 F I=1,NDW;S CI=I*WSS/TCAL;S CW(I)=TZ-CI
30.20 F I=1,NDW;S NW=NW1+1-I;DW NW,WT,CW(I)
31.05 T !," ENTER TIME ZERO CHANNEL ";A TZ;D 30
33.05 C SET UP WINDOW MARKERS FOR PLOT
33.10 T !,"REGION ";A NR;F J=1,NDW;USET NR,CW(J),1000
33.15 USET NR,TZ,1000
40.01 C DETERMINE THE CHANNEL OF THE HALF HEIGHT OF A COMPTON EDGE.
40.02 C   AN AVERAGE OVER "NAV" CHANNEELS ABOUT "C1","C2", DETERMINES THE PEAK
40.03 C   ANDD TAIL. A STRAIGHT LINE IS FITTED TO 1/5(C1-C2) CHANNELS ABOUT
40.04 C   THEE CLOSEST CHANNEL TO THE HALF HEIGHT, AND THE BEST VALUE FOUND.
40.08 T %10.02
40.09 T !," REGION ";A NR;T "  PEAK CHANNEL ";A C1;T "  TAIL CHANNEL ";A C2
40.10 T !," NUMBER OF CHANNELS FOR AVERAGING ";A NAV
40.15 S SM1=0;S SM2=0;F J=1,NAV;D 41
40.20 S HALF=((SM1+SM2)/2)/NAV;S J=C1
40.25 S J=J+1;IF (HALF-FGCH(J,NR))40.25,40.25,40.30
40.30 S CH=J;S NL=(C2-C1)/5;S CZ=CH-NL/2;S SY=0;S SXX=0;S SXY=0;S SX=0
40.31 S NL=FITR(NL);S CZ=FITR(CZ)
40.35 F J=1,NL;D 42
40.40 S M=(NL*SXY-SY*SX)/(NL*SXX-SX*SX);S B=(SY-M*SX)/NL
40.45 S XH=(HALF-B)/M+CZ;T !," HALF HEIGHT IS AT CHANNEL ",XH;S J=1;S CH=XH
40.50 D 12.10;D 12.20
41.05 S K=J-NAV/2+C1;S SM1=SM1+FGCH(K,NR)
41.10 S K=J-NAV/2+C2;S SM2=SM2+FGCH(K,NR)
42.05 S K=CZ+J-1;S Y=FGCH(K,NR);S X=J-1
42.10 S SY=SY+Y;S SX=SX+X;S SXX=SXX+X*X;S SXY=SXY+X*Y
44.05 T !,"REGION ";A NR;T "BACKGROUND MARKERS ";A C1,C2;S NL=C2-C1+1
44.10 S SM1=0;F J=C1,C2;S SM1=SM1+FGCH(J,NR)
44.15 S HAL=SM1/NL
44.20 T !,"CHANNELS DEFINING LINE ";A CZ,C2;S NL=C2-CZ+1
44.21 S SY=0;S SX=0;S SXY=0;S SXX=0;D 40.35;D 40.40;S CH=(HAL-B)/M+CZ
44.25 T !,"EXTRAPOLATED ZERO IS AT CHANNEL ",%1 .02,CH;D 10.03
50.01 DOFF
50.05 T !,"REGION ";A NR;A N;S P=N/M
50.10 F J=1,1023;S X=FGCH(J,NR)*R-FGCH(J,NR);USFT 11,J,X
50.15 DON
60.04 T %10.02
60.05 LM 0;HM HMS;LM LMS;DR 1,LMS,HMS
60.06 T !,"      REGION          AREA    C-TZ    (NS)    SIGMA NS"
60.10 F J=1,NW;DB J;D 61
61.05 INTR A,C,V,SD;S D=(C-TZ)*TCAL;T !,J,A,D,SD*TCAL,?
70.05 C COMPARE REGION R1 WITH R2 , NORMALISING TO CHANNEL CN AND COMPARING
70.06 C THIS RAATIO TO THE RATIO OF 510 OTHER CHANNELS
70.10 T !,"ENTER REFERENCE REGION ";A R1;T "   DATA REGION ";A R2
70.15 T !,"NORMALISE A CHANNEL ";A CN;T "UPPER CHANNEL ";A TL
70.20 D 72
71.05 F J=1,TL;S X=FGCH(J,R2)*Z/(FGCH(J,R1)+.01);USFT R2,J,X
72.05 S X=FGCH(CN,R1);S Y=FGCH(CN,R2);S Z=X*1000/Y
72.30 D 71
77.77 DOFF;T !,"DATA REGION ";A R2
77.80 D 72
77.85 DON
90.90T " CH ";A CH;T %10.02," TIME ",TCAL*(CH-TL),!
90.99 F J=1,20;D 90.90
91.05 IF (200000-J)91.10,91.10,91.15
91.10 T !,"END OF RUN ","********",!
91.15 T !,%10.00,J;D 7.05;D 2.05;T %10.02
99.99 T !,"SCALER OVERFLOW ";D 3.05;S CH=CHP;IPR JZ,CH,CH,J;D 91.05


END OF LISTING
```

APPENDIX B
THE TIME-DEPENDENT NEUTRON ENERGY SPECTRA

The following tables contain the neutron energy spectra for each time window, from both experiment and theory. Only the mid points of the energy groups and time windows are given. Full details of these are in Tables 2 and 3 respectively. The experimental results have been divided by 10^4. A scaling factor, F, is quoted with each of the theoretical spectra, which is the factor by which the raw theoretical spectra have been scaled. To obtain the best match to the experiment, a further scaling by 0.4 is required.

TABLE B1

EXPERIMENTAL TIME-DEPENDENT NEUTRON ENERGY SPECTRA

Energy (MeV)	0.8	1.25	1.75	2.25	2.75	3.25	4.0		5.0		5.95	
Time	Flux	Error = 10%						*E%		E%		E%
1.9	175.9	151.3	119.3	187.6	310.8	151.6	171.9	10	290.3	10	182.5	10
3.9	587.0	348.6	533.4	709.0	736.9	697.3	677.5		996.6		522.5	
5.9	1385	1376	1596	1230	1011	885.7	660.3		747.3		343.4	
7.9	2791	2479	1642	916.8	693.6	468.3	291.0		268.2		123.6	
10	3863	2348	1100	515.9	403.9	241.6	134.2		121.6		52.35	
12	3966	1819	681.1	310.7	223.3	128.2	67.58		54.13		27.70	
14	3699	1342	413.3	177.7	129.7	70.39	35.00		25.07		14.55	
16	3278	953.0	248.3	104.1	72.54	40.40	19.68		13.94		6.71	11
21	2233	400.2	74.90	31.94	20.74	14.39	5.41	11	3.90	12	1.88	14
26	1449	169.3	28.72	11.47	8.54	5.89	2.22	13	2.11	12	0.65	21
29.5	2703	243.8	40.43	19.16	13.10	9.99	4.05	11	2.67	12	1.60	14
34.5	1732	114.8	20.39	11.73	8.19	6.54	2.65	12	1.85	13	1.13	15
39.6	969.8	47.14	11.82	6.43	5.30	4.22	1.97	12	1.06	15	0.67	18
47.2	1013	43.64	15.74	10.23	8.38	6.25	3.03	12	1.72	13	1.08	15
57.2	405.6	20.99	10.52	9.61	5.61	5.39	1.17	17	3.06	11	0.01	13
67.2	167.5	14.70	9.52	7.66	5.31	3.86	2.01	12	1.13	15	0.90	15
77.2	80.3	13.94	8.21	7.88	9.11	4.48	2.05	12	1.05	15	0.61	20

*Percentage error

TABLE B2

MONTE CARLO CALCULATION OF TIME-DEPENDENT NEUTRON ENERGY SPECTRA

Energy (MeV)		0.8		1.25		1.75		2.25		2.75		3.25		4		5		5.95	
Time	Scale Factor x 10^{-12}	Flux	*E%	Flux	E%	Flux	E%	Flux	E%	Flux	E%	Flux	E%	Flux	E%	Flux	E%	Flux	E%
1.9	1.597	362.3	3	318.2	3	267.2	4	256.4	2	240.3	3	326.6	2	557.6	1	1098	1	358.2	3
3.9	1.250	1671	2	1515	2	1387	3	1408	2	1149	2	1329	2	1564	1	1966	1	546.5	6
5.9	1.329	5174	2	4643	1	3717	2	2911	2	1814	2	1529	2	1261	2	1011	2	296.6	7
7.9	1.261	11030	1	7010	1	3633	2	2221	2	1284	2	911.9	4	644.6	3	411.0	2	136.2	6
10	1.349	14920	1	5920	2	2383	2	1312	2	737.5	3	465.6	3	339.5	4	212.3	4	79.8	11
12	1.271	14290	1	4445	2	1495	3	766.3	3	414.9	4	266.5	5	191.9	5	113.3	7	42.3	9
14	1.176	12330	1	3032	2	880.6	3	446.8	3	227.5	4	171.6	10	114.2	8	58.3	8	22.2	8
16	1.089	10190	1	2030	2	527.1	3	267.4	4	138.0	5	95.4	10	64.8	8	34.4	5	13.4	9
21	1.009	6637	2	820.8	3	185.5	8	87.3	6	51.2	9	25.0	15	22.6	21	7.1	15	3.6	21
26	1.038	4497	2	376.7	4	66.6	8	31.7	15	17.0	14	7.2	20	5.6	17	4.0	48	2.0	45
29.5	1.093	8799	2	567.7	4	94.5	9	35.5	14	26.4	16	18.0	27	8.5	26	6.0	29	2.4	35
34.5	1.053	5189	2	255.7	6	50.8	14	24.3	21	12.7	22	8.6	27	3.9	26	2.6	30	1.8	40
39.6	0.878	3107	2	98.9	7	24.6	18	15.3	17	6.6	24	5.8	38	3.7	31	1.2	40	1.1	50
47.2	0.884	3080	3	96.5	10	33.9	21	19.3	19	20.8	27	12.8	26	5.9	24	3.1	37	0.5	66
57.2	0.866	1217	3	59.8	15	19.6	19	15.5	36	7.8	26	5.2	32	3.8	30	0.8	60	1.9	66

*Percentage error

Printed by the AAEC Research Establishment